Simultaneous S- and X-Band Uplink-Downlink Performance at DSS 13

A. J. Freiley
Radio Frequency and Microwave Subsystems Section

The DSS 13 26-meter antenna with the second generation S/X feedcone was tested to determine the dual S- and X-band (2.1 to 2.3 GHz and 7.1 to 8.5 GHz, respectively) transmit and receive performance. Measurements were conducted using the 20-kW transmitters at S- and X-band while simultaneously receiving S- and X-band. This system proved to be very quiet compared with the other DSN antennas. Under normal tracking configurations, no noise burst or intermodulation product (IMP) activity was detectable to the −175-dBm level. To prove the instrumentation's ability to detect such phenomena, an IMP generator was introduced onto the system with positive, verifiable results. The IMP occurred at the −162-dBm level, accompanied by moderate noise burst activity, and was readily repeatable. The measurement also showed the possible need for additional fourth-channel filtering in the system to reduce the effect of the transmitter power on the LNAs.

I. Introduction

In support of the deep space missions, the Deep Space Network has been developing systems capable of providing multiple uplinks and downlinks from a single antenna. Since the mid-1970s, the DSN has experienced occasional difficulty with the high-power/low-noise systems that are used for deep space communications. These systems simultaneously transmit from 20 kW to 500 kW and receive signals at the −160- to −170-dBm level. These systems occasionally experience problems with low-level corona, or arcing, which causes a momentary increase in system temperature, a phenomenon called noise bursts. Considerable effort has been expended to improve or eliminate the problem [3]. With the development of a dual uplink capability, the problems of intermodulation products present additional challenges to the operation of high-power/low-noise systems.

Initially, the dual uplink was attempted by trying to modulate a single klystron transmitter with two carriers. The systems were plagued with noise bursts, as well as with a general steady-state increase in the system noise temperature and higher-order intermodulation products (IMPs) caused by the nonlinear mixing of the two carrier signals. In this early work, the carriers were only a few megahertz apart, so the mixing products were also a few megahertz apart throughout the receive spectrum. The IMP frequency is generally stable, but the amplitude fluctuates rapidly over a wide range [1], [2].

Noise abatement efforts in the DSN [1] have improved the performance of the antennas greatly over initial conditions [2]. The systems are currently able to transmit a single 400- to 500-kW carrier with little or no noise burst activity, provided good antenna housekeeping techniques are maintained. How-

ever, the IMP problems caused by the dual-carrier transmission have never been overcome.

Advanced Transmitter Development personnel tested the new common aperture feed at DSS 13, called the XSR, to demonstrate its ability to transmit and receive two widely spaced signals simultaneously. The goal was to measure the level of performance in terms of noise burst and IMP levels, and to identify the various noise and IMP contributors, both internal and external to the feed system. The frequency bands of primary interest are 2110 to 2120 and 2270 to 2300 MHz at S-band and 7145 to 7135 and 8400 to 8500 MHz at X-band. In each case, the lower frequencies are the transmit band. Noise bursts and IMP generation are much reduced as a result of the widely separated transmit signals used in this system.

II. XSR System

The DSS 13 antenna is a 26-meter az-el Cassegrainian center-feed reflector. The feedcone [3] houses the microwave feed components, the X-band transmitter power amplifier, and the receiver front ends. The feed provides simultaneous S- and X-band transmission and reception. The S-band transmitter power amplifier is located in the electronics room behind the main reflector. The system performance characteristics are given in Table 1. Figure 1 is a functional block diagram of the XSR system. The feedhorn is a common aperture multimode corrugated horn. The feedhorn is followed by the S/X combiner, which separates the S- and X-band signals. The S-band signals are fed in radially, while the X-band signals pass directly through, into another corrugated section below.

A. X-Band System

The X-band system consists of a quarter-wave plate polarizer surrounded by round rotary joints that provide switchable RCP or LCP polarization. Following the polarizer is a round to rectangular transition. Next is a 54-dB coupler, which is the point at which the test transmitter signal is injected into the X-band system. The next component is a rectangular waveguide switch that is used to switch the input of the low-noise amplifier (LNA) from the horn to the ambient load to provide the absolute temperature reference for the measurement of the antenna system noise temperature (T_{op}).

The X-band diplexer consists of three components. The first is the junction which combines the transmit and receive signals. In the transmit arm, a filter prevents the noise power in the receive band from reaching the LNA. In the receive arm, another filter prevents the transmit signal frequencies from reaching the LNA.

Continuing down the system along the receive path, the next component is the LNA input coupler, which is used to inject test signals or the power from the noise diode assembly needed to measure T_{op}, Next is the cryogenically cooled X-band traveling wave maser. Its noise contribution to the system is 8 kelvins with an instantaneous bandwidth of 8 MHz; it is tunable through the range of 8400 to 8500 MHz. The amplified signal is then distributed or switched to one of three receivers. There are two modified Block III receivers, one of which can be configured to X-band. There is also an R&D receiver, which consists of a simple mixer/downconverter assembly, and a radar receiver used to condition the radar signals. The modified Block III receiver and the R&D receiver proved the most useful for supporting the measurements reported here. The output of each of the receivers is a standard 50-MHz signal that is distributed to various locations in the station.

The X-band transmitter portion of the system is driven by a synthesizer. The signal is multiplied by 336, amplified, and fed into the transmitter power amplifier. The RF signal passes through a harmonic filter to reduce levels of unwanted signals. Then the filtered signal is fed into the transmitter port of the diplexer and radiated out the horn.

B. S-Band System

The S-band signals emerge from the combiner into the labyrinth waveguide assembly. This assembly consists of four equal-length waveguide runs, two waveguide magic tees, and a short slot hybrid. This waveguide assembly functions as a polarizer. An S-band RCP signal is received into the horn and the energy is coupled into the waveguide. The labyrinth phases the four signals in such a way as to produce a linearly polarized fundamental mode in the rectangular waveguide feeding the first waveguide switch. This switch selects either the low-noise listen-only receive configuration or the somewhat higher noise diplexed configuration. For the purpose of the system tests, the diplexed configuration was required.

The S-band diplexer consists of a short slot hybrid to combine or separate the transmit and receive signals and a filter section of waveguide below cutoff to allow the receive signal to propagate through while attenuating the transmit signal (thus protecting the LNA from the high power). The receive signal is combined in another short slot hybrid and then propagates through another waveguide switch that selects between the diplexed configuration and the S-band ambient load. The next component is the WR430 X-band reject filter, which protects the S-band LNA from X-band transmitter power that may couple into the S-band waveguide system. The multiport LNA input coupler allows the injection of signal and noise diode power to calibrate the receive system. The S-band low-noise amplifier is a cryogenically cooled traveling wave maser that contributes 2.5 kelvins to the system. The amplified signal is distributed to the applicable receiver.

The S-band transmit signal is based on a synthesizer signal that is multiplied by 48 and fed into the transmitter power amplifier. The high-power RF signal then passes through a low-pass filter to reduce the levels at the receive frequencies, and through a harmonic filter to reduce the harmonic level to avoid interference in the X-band system. This filtered signal is then passed to the diplexer and out the horn.

III. Noise Instrumentation

The station noise instrumentation consists of three sets of equipment. The first is the conventional Y-factor instrumentation. The 50-MHz signal from the receiver passes through an AIL variable attenuator to the power meter detector. The power meter detector feeds a DC voltage to a stripchart recorder.

The second set of equipment is the noise-adding radiometer (NAR). The 50-MHz signal from the receiver is fed into the square-law detector, where the power is converted by a voltage-to-frequency converter. This proportional frequency is fed into a frequency-to-digital converter within the NAR to calculate the system temperature based on the strength of the noise diode power injected into the microwave system (see Fig. 1).

The third set of equipment is a subset of the NAR system. The 50 MHz are fed into the square law detector as in the previous set, but the detector also has a DC output that is proportional to the input power. This DC signal is displayed on a stripchart recorder. Through the use of the noise diodes, the stripchart can be calibrated in kelvins per inch.

Both the Y-factor instrumentation and the NAR instrumentation produced the same results when measuring the system temperature of the S-band and X-band systems, even though each set of instrumentation derives its results by a different method. This agreement indicates that the receiving system is linear. (The results of these measurements are given in Table 1.) However, each of these sets of instruments disrupts or masks the measurements of the noise burst activity and the IMP detection. The simplest instrumentation, the square-law detector and stripchart recorder, proved to be the best for monitoring the noise burst activity.

IV. IMP Predictions

The amplitude of the IMP signals is a quantity that is unpredictable with any accuracy. Previous measurements have encountered levels typically about −140 dBm for the order $N = 31$. For the measurements at hand, the order was much lower, and therefore one might expect the levels to be stronger if all else were equal. The intermodulation product frequency (F_i) is predictable by the following equation:

$$F_i = mF_x + nF_s$$

where F_x is the frequency of the X-band transmitter signal, F_s is the frequency of the S-band transmitter signal, and m and n are the indication of the order of the intermodulation by the following equation:

$$\text{intermodulation order} = m + n$$

For the transmitter frequencies of 2110 and 7173 MHz, S-band and X-band respectively, and $m = 5$ and $n = 13$, the frequency of the IMP will be 8435 MHz.

V. Test Procedure

During the system tests, each session would generally follow the steps listed below. Some variations would result if some phenomenon occurred. Items 9 through 14 are some of the variations that were attempted.

(1) Configure system.

(2) Measure the S-band and X-band system noise temperatures.

(3) Configure test signals for both S and X.

(4) Calibrate test signal.

(5) Measure or observe spectrum with and without signals to determine signal strength.

(6) Radiate 20 kW from S-band transmitter only. Note any changes in the system.

(7) Radiate 20 kW from X-band transmitter only. Note any changes in the system.

(8) Simultaneously radiate 20 kW from each transmitter. Note any changes in the system.

(9) Sweep S-band transmitter while X-band remains fixed. Note any changes.

(10) Sweep X-band transmitter while S-band remains fixed.

(11) Perform antenna tipping curve with both transmitters radiating.

(12) Apply modulation signals.

(13) Move the antenna in azimuth and/or elevation and apply brakes.

(14) Install the "surefire" noise generator (described below).

(15) Vary the amplitude of one transmitter or the other.

VI. Results

Each measurement session began by configuring the station to ensure consistency. The measurements of T_{op}, maser gain, and receiver follow-up temperature were the primary parameters used to determine if the system was configured consistently with previous sessions. The noise temperature was typically about 31 kelvins at S-band and 28 kelvins at X-band. The maser gain was set to 45 dB, and the follow-up temperature was usually under 0.1 kelvin for each receiving system, depending on the receiver used.

Early in the sessions, the S- and X-band R&D receivers were used with the spectrum analyzer installed in the maser instrumentation rack with no visible results such as noise burst or IMPs. Previous measurements as reported in [2] were visible with this instrumentation. No matter what was done, no noise bursts or IMPs were detected. The fourth harmonic of the S-band transmit signal was observed at 8440 MHz, which correlates with the 2110-MHz S-band transmitter signal. When the S-band frequency was tuned up 1 MHz, the harmonic would move up 4 MHz.

The next approach was to use the Block III receiver and slowly search through the range of frequencies where an IMP was predicted, based on the calculations, in an attempt to lock the receiver to an IMP and measure its amplitude and frequency. No positive results were obtained, although the fourth harmonic was easily detected. The test transmitter signal could also be easily detected. Much difficulty was encountered in maintaining a consistent system configuration for the duration of these tests. As is the nature of a research and development station such as DSS 13, equipment is changed or modified and the capabilities are changed over a period of time. Such was the case with the Block III receiver; some modified modules were installed, leaving the receiver unable to lock to a signal. Restoration of the capability could not be accomplished in a timely manner, so the Block III receiver testing was abandoned.

In the continuing search for some indication of noise burst and IMP activity, the R&D receiver was drafted back into service with the addition of the SETI digital spectrum analyzer [4] to increase the sensitivity of the receiving system. The digital spectrum analyzer bandwidth covers 20 MHz, divided into two windows of 10 MHz each. The analyzer divides that bandwidth into 2^{16} (65,536) channels, each channel representing a bandwidth of 305 Hz. The integration time for a single measurement is 3.3 msec. The total integration time is adjustable with input to the computer controlling the spectrum analyzer. With this system and about 6 seconds of integration time, the system threshold was −175 dBm. The spectrum display that provided the clearest indication of noise was developed by measuring the peak amplitude in each channel.

Figure 2 shows a sample of the spectrum from 8431 to 8441 MHz. Directly in the center is the "DC line" (an artifact of the instrument) and to the left of center is a signal that corresponds to the X-band test transmitter signal at 8433 MHz at an amplitude of approximately −162 dBm. During this test, there was no radiated RF power in the system. With each of the transmitters radiating 20 kW, S-band at 2110 MHz and X-band at 7173 MHz, the spectrum of Fig. 3 shows the addition of the fourth harmonic of the S-band at 8440 MHz (four times 2110). The amplitude was strong enough to saturate that channel of the spectrum analyzer, so no accurate amplitude measurement was obtained. During this period, no noise bursts were recorded and no IMPs detected. It was not the purpose of these tests to eliminate the fourth harmonic signal; should it prove troublesome in the future, it would yield to standard RFI prevention techniques.

In an attempt to find and measure some evidence of noise bursts and intermodulation activity, the "surefire" IMP generator was created. It consisted of a large aluminum pipe clamp, a rusty bearing and chain, aluminum shavings, and aluminum wire woven through the steel chain. This unusual collection of material was suspended from the quad leg about 4 feet above the dish. A rope was attached and fed down through the dish, allowing station personnel to mechanically disturb the IMP generator to increase its effectiveness in generating noise bursts and IMPs. Given the operating frequencies above, the IMP should have appeared at 8435 MHz, and the spectrum of Fig. 4 shows a signal at 8435. The test signal was adjusted in amplitude to match the IMP level and then measured to be −162 dBm. The S-band and X-band transmitters were radiating at 20 kW and the IMP generator was shaken during the integration period. The fourth harmonic signal also increased.

Figure 5 presents a clear record of the activity of the total noise power as the test progressed through the series just described. Area A shows the noise power with no RF power radiated. The level of the X-band trace was adjusted to provide a clear picture of the activities in each channel. Area B shows each transmitter coming up to full power with the accompanying momentary disturbance. Note the level changes that are most likely caused by a small amount of transmitter power getting into the LNAs, thus increasing the total system noise power and/or affecting the gain of the LNA. Note that the sensitivity of the recording at X-band is 2.3 kelvins per inch and at S-band is 3.5 kelvins per inch. Also, note that the general momentary response (trace jitter) of each trace did not change with or without the RF power. As the radiated power was shut off, the traces shifted back in the same direction as before the power was applied.

Area C shows the system response to the installation of the IMP generator on the dish. The X-band temperature increased

approximately 1.7 kelvins and the S-band temperature increased approximately 1.4 kelvins due to personnel on the reflector surface. Area D shows a dramatic increase in noise burst activity. Also detectable is the shift in the baseline level, as was seen before without the IMP generator installed. Areas E and F show the increase in activity as the IMP generator was disturbed mechanically. The level increases at both S- and X-band, denoting an increase in system noise temperature and noise burst activity. When the shaking ended, the traces returned to the same levels as before. During these shaking periods, the IMPs were measurable, as seen in Fig. 5.

Area G shows that the S-band system temperature returned to the same pre-transmitter condition when the S-band transmitter interlock automatically shut down the transmitter. When the transmitter came back to full power, the noise bursts also returned, as can be seen in Area H. Following Area H, one additional shaking period of the IMP generator occurred. Next, when the IMP generator was removed from the dish, the presence of personnel on the dish caused a corresponding increase in temperature (Area I). Area J shows performance with each transmitter back up to the full 20 kW but without the IMP generator. This compares well with the previous recordings of Area B.

VII. Conclusions

The common aperture feed at DSS 13 is free of noise bursts and of intermodulation product signals down to the −160- to −170-dBm levels. The instrumentation used for the measurements is capable of detecting activities at that level if they are present, as demonstrated by the artificial IMP generator tests.

Two factors contribute to this good performance. The first is the nature of the feed. The point at which both the S-band and X-band signals are combined is high in the feed, thus exposing few components to the RF power from both transmitters and limiting the opportunities for creating intermodulation products. The second factor is the excellent general "housekeeping" of this antenna. The feed is kept clean and free of foreign matter that contributes to arcing and mixing of signals. The reflecting surfaces of the antenna are free of loose items or marginally clamped items that could provide the nonlinear situations necessary for creating IMPs.

The system does demonstrate the possible need for additional RF filtering to reduce the levels of the fourth harmonic and to reduce the beam noise that apparently is seen by both LNAs. Additional measurements would be required to determine amplitudes and the corresponding filtering requirements.

References

[1] D. A. Bathker, D. W. Brown, and S. M. Petty, *Single- and Dual-Carrier Microwave Noise Abatement in the Deep Space Network*, Technical Memorandum 33-733, Jet Propulsion Laboratory, Pasadena, California, August 1, 1975.

[2] R. C. Chernoff and R. W. Hartop, "Noise and Intermodulation Interference in MSFN Back-up Tracking Systems During Transmission of Dual Uplink Carriers," *Deep Space Network Space Progress Summary 37-57*, vol. II, Jet Propulsion Laboratory, Pasadena, California, pp. 138–145, May 31, 1969.

[3] J. R. Withington, "Second-Generation X/S Feedcone, Layout and Components," *TDA Progress Report 42-63*, vol. March–April 1981, Jet Propulsion Laboratory, Pasadena, California, pp. 97–103, June 15, 1981.

[4] G. A. Morris, and H. C. Wilck, "JPL 2^{20} Channel 300-MHz Digital Spectrum Analyzer," *Proc. IEEE International Conf. of Acoustic, Speech, and Signal Processing*, pp. 808–811, 1978.

Table 1. XSR system performance characteristics

Characteristics	S-band	X-band
System temperature	31 K	28 K
Receiving bandwidth	10 MHz	8 MHz
Tunable	2270–2300 MHz	8400–8500 MHz
IF frequency	50 MHz	50 MHz
Transmitter power	20 kW	20 kW
Tunable bandwidth	2110–2120 MHz	7145–7235 MHz

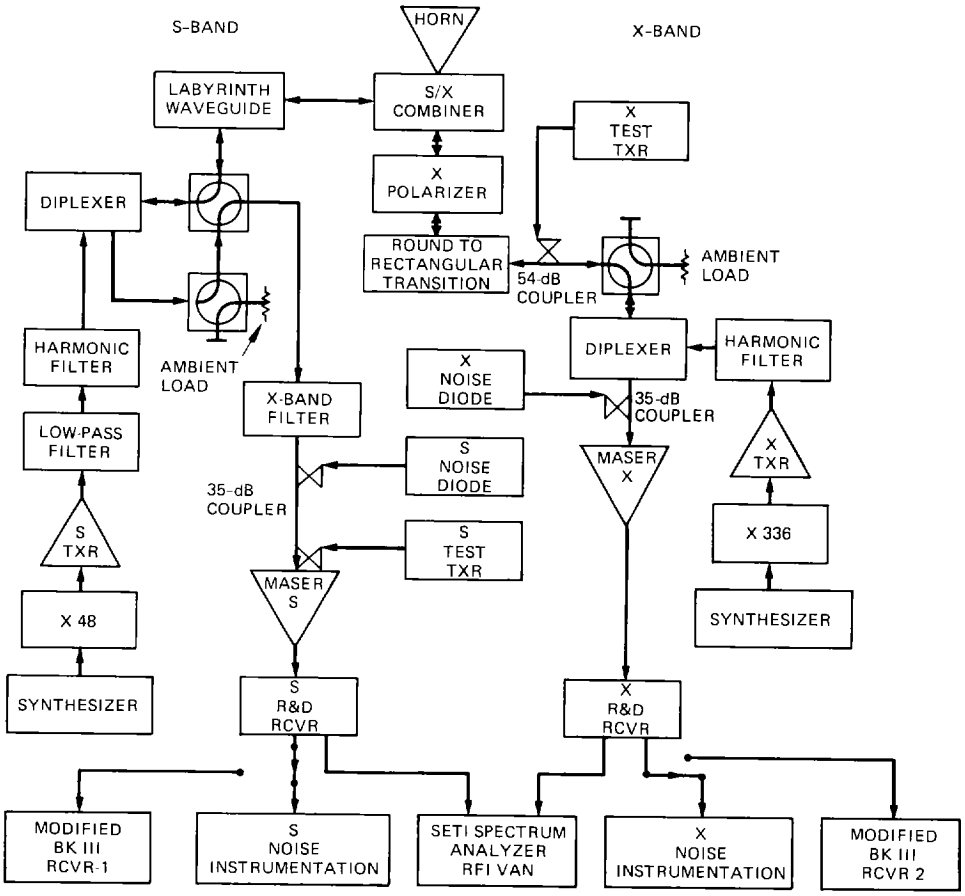

Fig. 1. XSR system functional block diagram

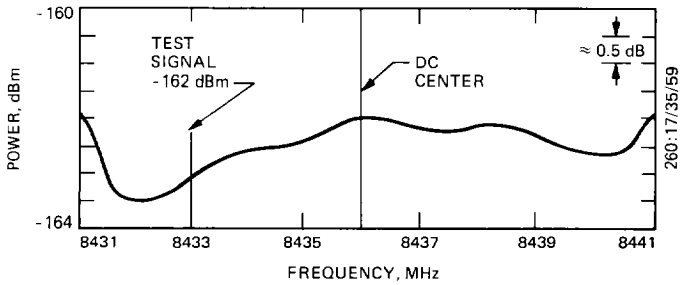

Fig. 2. X-band receive spectrum with locally injected test signal (no transmitter RF power)

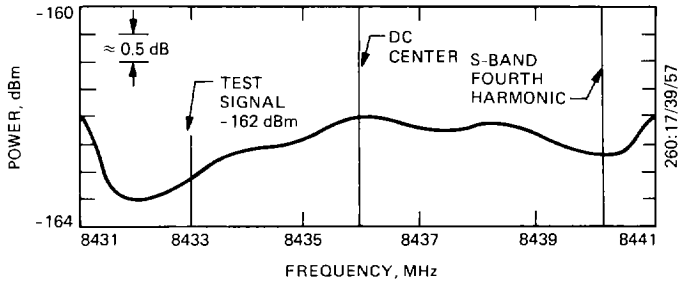

Fig. 3. X-band receive spectrum with S- and X-band transmitters each radiating 20 kW

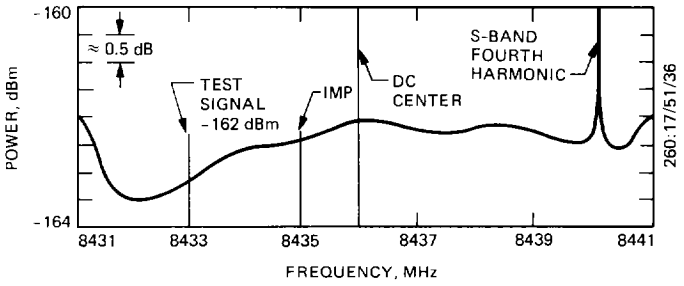

Fig. 4. X-band receive spectrum with artificial IMP generator on the dish surface

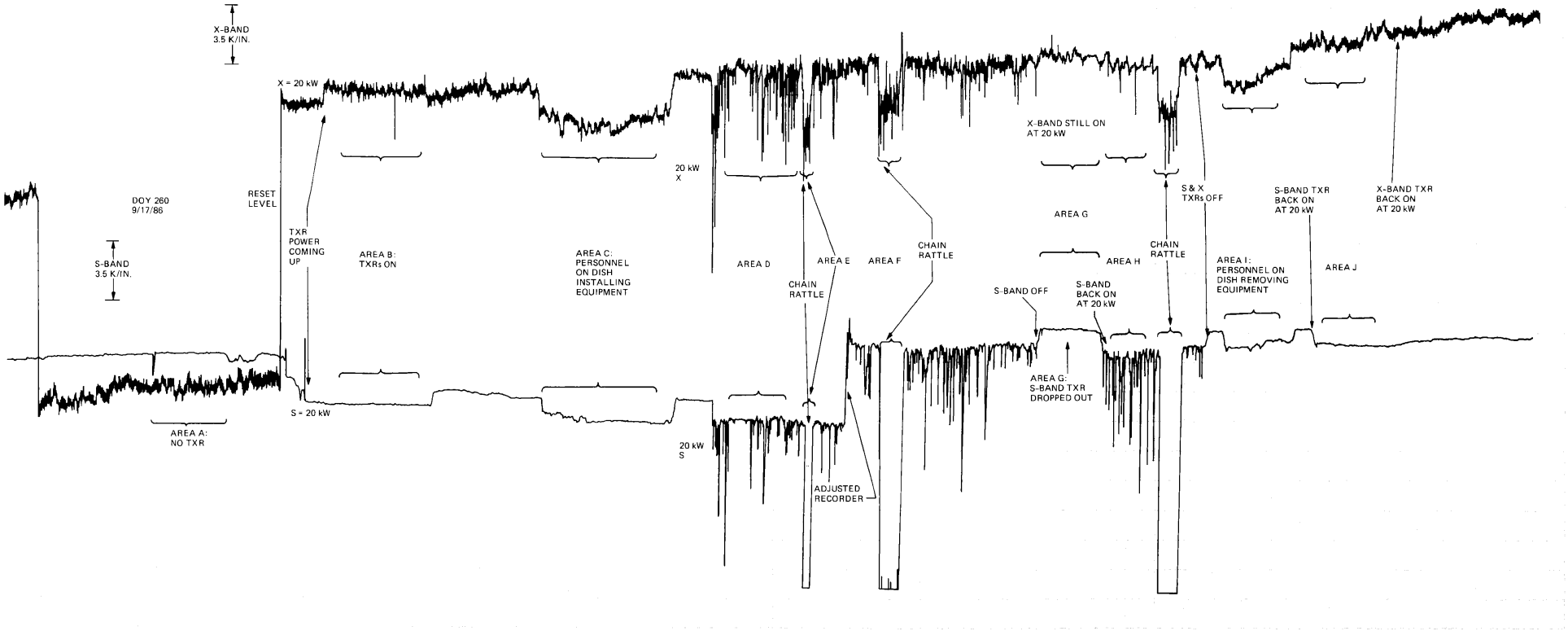

Fig. 5. Total system noise power stripchart recording